

BBAMEM 75903

Regulation of inositol 1,4,5-trisphosphate receptors in rat basophilic leukemia cells. I. Multiple conformational states of the receptor in a microsomal preparation

F. Charles Mohr ^a, Panda E.C. Hershey ^a, Ildikó Zimányi ^b and Isaac N. Pessah ^b

^a Department of Veterinary Pathology, University of California, Davis, CA (USA) and ^b Department of Pharmacology and Toxicology, University of California, Davis, CA (USA)

(Received 4 November 1992)

Key words: Calcium store; Intracellular calcium regulation; Inositol 1,4,5-trisphosphate; Mast cell; RBL cell

A detailed characterization of the inositol 1,4,5-trisphosphate (IP₃) receptor in rat basophilic leukemia (RBL) cells, a neoplastic mast cell line, has been possible through the growth of solid RBL cell tumors which provide a rich source of IP₃ receptor. Equilibrium binding studies show a 1.6 ± 0.1 pmol/mg of protein maximal binding capacity for [³H]IP₃ at optimal Ca²⁺ (10 μM). The specificity of the RBL cell IP₃ receptor towards phosphoinositides, ATP and heparin parallels those previously described with excitable and nonexcitable tissues. [³H]IP₃ binding is slightly enhanced from < 1 nM to 10 μM Ca²⁺ and inhibited by > 10 μM Ca²⁺. Kinetic and equilibrium studies provide evidence for at least two classes or conformational states of binding sites with pico- and nanomolar affinities. At nM concentrations of IP₃, neither binding to the IP₃ receptor nor IP₃-induced Ca²⁺ efflux from permeabilized cells demonstrates cooperativity. In contrast, at pM concentrations, IP₃ binding kinetics deviate from simple mass action suggesting a complex interaction among binding sites for IP₃ on the receptor-channel oligomer. The mechanisms that regulate [³H]IP₃ binding in RBL cells are unique when compared to what has been reported in other cells.

Introduction

Inositol 1,4,5-trisphosphate (IP₃), one of the products of receptor-mediated hydrolysis of phosphatidylinositol 4,5-bisphosphate, acts as an intracellular messenger by mobilizing Ca²⁺ from an intracellular store [1]. The intracellular receptor for IP₃ is coupled to a calcium (Ca²⁺)-release channel [2] with structural and functional properties resembling those of the ryanodine receptor-Ca²⁺ release channel complex of the triadic junctions of striated muscle [3]. Intracellular binding sites exhibiting low nanomolar affinity for IP₃ have been characterized from subcellular fractions of a variety of excitable cells, e.g., nerve [4–6], smooth muscle [7], endocrine [8–10], and nonexcitable cells, e.g., hepatocytes [11–14]. Only a few reports have

documented radiolabeled IP₃ binding in bone marrow-derived cells such as permeabilized neutrophils [15], mast cell microsomes [16], platelet membrane vesicles [17], and HL-60 cells, a cell line of leukemic promyelocytes [18].

IP₃ binding to an intracellular receptor is regulated by various physiological modulators. The specific binding of [³H]IP₃ is enhanced by alkalization in a variety of cell types [4,7,10,17]. Concentrations of free ionized Ca²⁺, known to be attained in agonist-stimulated cells, inhibit the binding of [³H]IP₃ to cerebellar membranes [4,19] but enhance binding to hepatocyte plasma membrane fractions [14]. Lastly, ATP inhibits [³H]IP₃ binding with concentrations of ATP resulting in half-maximal inhibition (IC₅₀) in or near the millimolar range [9,10,20].

The rat basophilic leukemia (RBL) cell line is derived from transformed mast cells [21]. When stimulated with specific antigens, immunoglobulin E-sensitized RBL cells produce IP₃ [22], increase the cytoplasmic concentration of Ca²⁺ [23,24], and secrete mediators of immediate hypersensitivity [25]. The presence of intracellular Ca²⁺ stores has been demonstrated in RBL cells [24], and release of Ca²⁺ from these stores may be important in antigen-mediated secretion [26].

Correspondence to: F.C. Mohr, Department of Veterinary Pathology, University of California, Davis, CA 95616, USA.

Abbreviations: B_{max}, maximum number of binding sites; EC₅₀, concentration resulting in 50% of the maximal effect; IC₅₀, concentration resulting in 50% inhibition; IP₃, inositol 1,4,5-trisphosphate; K_d, dissociation constant; k₊₁, association rate constant; k₋₁, dissociation rate constant; k_{obs}, observed association rate constant; n_H, Hill constant; RBL, rat basophilic leukemia.

Meyer and co-workers have demonstrated that permeabilized RBL cells contain a pool of intracellular Ca^{2+} which releases Ca^{2+} by an IP_3 -sensitive mechanism [27,28]. Analysis of their kinetic Ca^{2+} efflux experiments suggests that there are multiple independent binding sites for IP_3 but that IP_3 -induced Ca^{2+} release involves a cooperative mechanism, suggesting a complex interaction between IP_3 and its binding sites on the intracellular IP_3 receptor- Ca^{2+} channel complex.

The major obstacle to the elucidation of structure-function relationships of the IP_3 -activated Ca^{2+} channel in bone marrow-derived cells is the lack of sufficient biological material for detailed biochemical characterization. These limitations are circumvented in the RBL cell line because subcutaneous administration of cultured RBL cells into neonate rats produces gram quantities of solid RBL cell tumors. We utilize solid RBL cell tumors to identify a microsomal fraction that is enriched in specific $[^3\text{H}]\text{IP}_3$ receptor sites. In this paper we characterize the IP_3 receptor in this neoplastic cell line and demonstrate unique features not previously attributed to IP_3 receptors found in other tissues.

Materials and Methods

Cells. Binding studies were performed with a microsomal fraction of a secreting cell line (2H3) of rat basophilic leukemia cells [21] grown as solid tumors, and Ca^{2+} efflux experiments were performed with the same cell line maintained in monolayer culture as previously described [29].

Reagents. D-[1- ^3H]Inositol 1,4,5-trisphosphate (17 Ci/mmol, 99% purity) was purchased from Du Pont-New England Nuclear (Wilmington, DE). Inositol 1,4,5-trisphosphate and inositol 2,4,5-trisphosphate were purchased from Calbiochem (San Diego, CA). ATP and *myo*-inositol biphosphate, low molecular weight heparin, and de-N-sulfated heparin were from Sigma (St. Louis, MO). Reduced streptolysin O was purchased from Wellcome Reagents, (Greenville, NC), and fluo-3 was from Molecular Probes (Eugene, OR).

Preparation of RBL cell solid tumors and microsomes. Cultured cells were suspended in cell culture media without serum or antibiotics and were injected subcutaneously (approx. $(8-10) \cdot 10^6$ cells/animal) into 2 week old Wistar rats (Tac:N(WKY)fBR; Taconic Farms). Ten days later the rats were killed, and the tumors were harvested. Dissected tumors were immediately frozen in liquid N_2 and stored at -70°C .

RBL cell tumors (40 g) were allowed to partially thaw before the tissue was finely minced and homogenized with 8 volumes of ice-cold homogenization solution composed of 110 mM KCl, 10 mM NaCl, 5 mM KH_2PO_4 , 2 mM MgCl_2 , 2 mM EGTA, 1 mM dithiothreitol, and 20 mM Hepes (pH 7.2) in a Waring Blender (3–5 s at maximum speed). The filtered ho-

mogenate was subjected to centrifugations at 4°C in the following sequence: 20 min at $1500 \times g$, supernatant for 10 min at $8000 \times g$, and supernatant for 20 min at $35000 \times g$. The $35000 \times g$ pellet was washed once in EGTA-free homogenization buffer and repelleted. The final pellet was resuspended with a loose-fitting Dounce homogenizer in 25 mM Na_2HPO_4 , 1 mM EDTA, 10% sucrose, 0.1% BSA (pH 7.4) portioned in 0.5 ml aliquots, and quickly frozen in liquid N_2 . Protein concentrations were determined by the method of Lowry et al. [30].

The $35000 \times g$ pellet was enriched 6-fold in $[^3\text{H}]\text{IP}_3$ binding capacity when compared to the filtered homogenate. Electron microscopic examination showed the composition of the receptor-enriched fraction to be predominantly membrane vesicles up to 40 nm in diameter (designated as microsomes) with minor contaminants of mitochondria and secretory granules.

$[^3\text{H}]\text{IP}_3$ binding to RBL cell microsomal membranes. Equilibrium experiments were performed with approximately 600 μg of protein and 0.2–0.5 nM $[^3\text{H}]\text{IP}_3$ (17 Ci/mmol) in a total volume of 1 ml of assay solution containing 100 mM KCl, 20 mM NaCl, 1 mM EDTA, 0.1% BSA, 25 mM Na_2HPO_4 (pH 8). Assays were performed at 4°C with constant shaking. Non-specific binding was measured in the presence of a 100-fold excess of unlabeled IP_3 . Equilibrium binding reactions were terminated after 30 min by rapid, single manifold filtration through Whatman GF/B filters pre-soaked in ice-cold assay solution. The filters were immediately washed with 2.5 ml ice-cold assay solution; the entire process required fewer than 5 s per sample. Filters were placed in Ready Safe scintillation cocktail (Beckman) and counted in a scintillation counter (Beckman) with an efficiency of 43%. In a typical experiment, specific binding was about 1800 dpm, while non-specific binding was generally 10–15% of total binding.

Binding experiments were also performed using centrifugation to terminate the reaction. These experiments were performed with 500 $\mu\text{g}/\text{ml}$ microsomal protein and 0.5 nM $[^3\text{H}]\text{IP}_3$ in a total volume of 250 μl of the assay solution described above in 400 μl -capacity polyethylene microfuge tubes. Reactions were incubated at 4°C for 30 min and were terminated by centrifugation at $50000 \times g$ for 20 min. The supernatant was removed and the portion of the tube containing the microsomal pellet was placed in scintillation fluid and counted for radioactivity. Non-specific binding was measured in the presence of a 100-fold excess of unlabeled IP_3 .

To examine the effect of free Ca^{2+} or Mg^{2+} on equilibrium binding of $[^3\text{H}]\text{IP}_3$, the free divalent cation concentration was adjusted with EDTA using the stability constants published by Fabiato [31] and calculated with the SPECS computer program.

Association experiments were performed by termi-

nating the binding of [^3H]IP $_3$ (0.2–0.4 nM) to microsomes at 4°C at times ranging from 0.15 to 90 min by rapid filtration. Dissociation of [^3H]IP $_3$ from the microsomal binding site by competition with unlabeled ligand was determined by equilibrating [^3H]IP $_3$ (0.2–0.4 nM) with microsomes for 30 min at 4°C and then adding a 100-fold excess of unlabeled IP $_3$ to the incubation mixture. Dissociation of [^3H]IP $_3$ from the microsomal binding site by dilution with excess assay solution was determined by equilibrating [^3H]IP $_3$ (3–4 nM) with microsomes in a total volume of 100 μl of assay solution and then adding a 100-fold excess of ice-cold assay solution to the incubation mixture. Residual specific binding was measured from 0.15 to 90 min by rapid filtration. In both association and dissociation experiments non-specific binding did not vary with time.

Ca $^{2+}$ release from permeabilized cells. Streptolysin O was used to permeabilize cultured RBL cells, and free ionized Ca $^{2+}$ was measured with the calcium-sensitive fluorescent dye fluo-3 [32]. RBL cells were initially washed twice in a saline solution composed of 135 mM NaCl, 5 mM KCl, and 10 mM Hepes adjusted to pH 7.2 with NaOH. The cells were then resuspended to $2 \cdot 10^6$ cells/ml in a simplified saline solution composed of 140 mM KCl and 30 mM Hepes (pH 7.2), adjusted with KOH. Fluo-3 (1 μM) was added to the cells, and 3 ml of the cell suspension was placed in polystyrene cuvettes maintained at 18–19°C in a thermostatted cuvette holder and constantly stirred by a small magnetic bar. Streptolysin O (0.2–0.4 units/ml) was subsequently added, and membrane permeabilization was monitored by a decrease in fluorescence and by the extent of Trypan blue staining in aliquots of cells. Experiments were started when the decline in fluo-3 fluorescence had leveled off and greater than 90% of the cells stained with Trypan blue. Care was taken to ensure rapid and complete mixing of added agents. Fluorescence was measured with a Perkin-Elmer LS-5B fluorescence spectrophotometer (excitation 506 nm, emission 526 nm). The free ionized Ca $^{2+}$ concentration was determined by the relationship [33]

$$[\text{Ca}^{2+}] = K_d(F - F_{\min}) / (F_{\max} - F)$$

where $K_d = 450$ nM (value given by Molecular Probes, Eugene, OR), F was the measured fluorescence intensity, F_{\max} was the fluorescence in the presence of excess Ca $^{2+}$ (2 mM), and F_{\min} was the fluorescence in the absence of Ca $^{2+}$ (20 mM Tris base, 20 mM EGTA).

Analysis of data. Data obtained from equilibrium binding experiments were analyzed using the computer program LIGAND. Data obtained from kinetic binding studies and from Ca $^{2+}$ efflux experiments were analyzed using the nonlinear regression computer program ENZFITTER. In calculating kinetic constants obtained

from association and dissociation studies, no correction was included for hydrolysis of [^3H]IP $_3$ since previous work by Guillemette et al. [34] has shown that the stated assay conditions both optimize IP $_3$ binding and minimize its degradation. Assays were also performed at 4°C and in the absence of Mg $^{2+}$ in order to minimize hydrolysis of [^3H]IP $_3$ by phosphatases [35]. In addition, the consistent observation that binding was stable for at least 60 min indicated that hydrolysis of IP $_3$ was not a significant factor. In the Ca $^{2+}$ efflux assays, previous work by Meyer et al. also indicated that under comparable assay conditions, no hydrolysis of IP $_3$ occurred within 10 min [27].

Results

Characteristics of [^3H]IP $_3$ binding in an RBL cell microsomal fraction

Specific binding of [^3H]IP $_3$ to RBL cell microsomes is proportional to the protein concentration in the assay medium and is reduced to non-specific levels by heat treatment (50°C, 10 min) or by digestion with trypsin (10 $\mu\text{g}/\text{ml}$) (unpublished data). Binding performed at low (< 1 nM) free Ca $^{2+}$ and Mg $^{2+}$ is saturable in the range of 0.5 to 10 nM IP $_3$ (Fig. 1) and is resolved into a single class of binding sites having nanomolar affinity (apparent $K_d = 1.5 \pm 0.3$ nM) and a capacity (B_{\max}) of 0.9 ± 0.1 pmol/mg protein (mean and S.D. of three independent experiments performed at pH 8.0). When centrifugation is used instead of filtration to terminate the binding reaction, comparable values for the apparent K_d and B_{\max} are obtained: 3.3 nM and 2.4 pmol/mg protein, respectively. [^3H]IP $_3$ receptor occupancy increases 4.25-fold with alkaliniza-

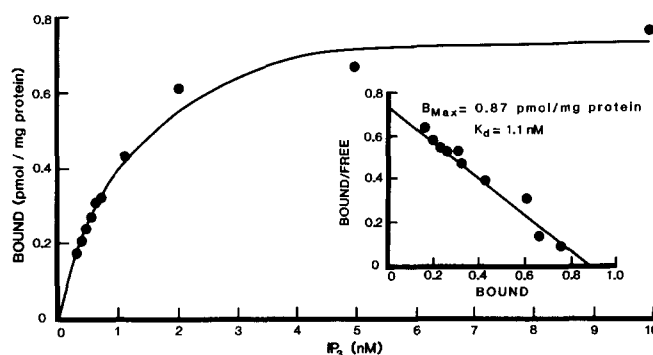


Fig. 1. Equilibrium binding analysis of [^3H]IP $_3$ to RBL cell microsomal membranes. The experiment is performed by adding unlabeled IP $_3$ (0.1–10 nM) to a fixed amount of [^3H]IP $_3$ (0.4 nM) and measuring specific binding under equilibrium conditions. The dpm of specific radioligand binding are transformed into pmol/mg protein. The free Ca $^{2+}$ and Mg $^{2+}$ concentrations in this experiment are less than 1 nM. Inset: Scatchard analysis of the binding data. The data are from one experiment and are representative of three separate experiments performed in duplicate at pH 8.0.

tion in the pH range of 6.0 to 8.0 (from 0.02 to 0.085 pmol/mg protein; measured at 0.4 nM [^3H]IP $_3$).

[^3H]IP $_3$ binding sites having lower affinity have been identified in cerebellum [5] and liver [11,13]. These low affinity sites are not present on RBL cell microsomal membranes since saturation experiments performed with 5 nM [^3H]IP $_3$ and competing concentrations of unlabeled IP $_3$ ranging from 5 to 100 nM show that occupancy within this range of IP $_3$ concentrations is already fully saturated (unpublished data).

When [^3H]IP $_3$ equilibrium binding experiments are performed with [^3H]IP $_3$ concentrations extending from 0.025 to 10 nM, the binding of [^3H]IP $_3$ to RBL cell microsomal membranes is no longer to a single class of sites. Instead the convexity of the Scatchard plot of the equilibrium data (Fig. 2A) indicates that the binding of IP $_3$ to its receptor in this range of ligand concentrations displays complex behavior. Specific [^3H]IP $_3$ binding can be discriminated from non-specific binding at concentrations as low as 25 pM [^3H]IP $_3$ (total dpm: 355 ± 22 , nonspecific dpm: 166 ± 22). The convexity of the plot is not attributed to the failure to achieve equilibrium binding conditions at the lower [^3H]IP $_3$ concentrations. Based on a k_{-1} of 0.003 s^{-1} (slow phase of dissociation by dilution, Table I), the half-time of steady-state binding is 3.8 min. The 30 min incubation period of the equilibrium experiment represented by Scatchard analysis in Fig. 2A reflects approx. 8 half-lives demonstrating that even at low concentrations of [^3H]IP $_3$, the experiments represented by Fig. 2A are performed under equilibrium conditions. The curvilinear result in Fig. 2A prevents extrapolation of the K_d values and B_{max} values for the higher affinity binding sites; by computer analysis the Hill number is 1.5. A double-reciprocal plot of the IP $_3$ concentration vs. the amount of [^3H]IP $_3$ bound is also curvilinear (Fig. 2B). However, when the IP $_3$ concentration is raised to the 1.5 power before the reciprocal is taken, the relationship becomes linear, $r = 0.99$, (Fig. 2B), in agreement with a Hill number in the range of 1.5.

Association and dissociation kinetic studies

The mechanism responsible for the complex binding behavior at very low concentrations of [^3H]IP $_3$ demonstrated in Fig. 2 may be due to transitions of the IP $_3$ receptor into different conformational states induced by increasing IP $_3$ concentration. This is demonstrated by kinetic binding experiments performed with RBL cell microsomal membranes (Fig. 3). Association studies by rapid, single manifold filtration reveal a very rapid association of [^3H]IP $_3$ with its binding site ($k_{\text{obs}} = 0.046 \text{ s}^{-1}$) which reaches maximal binding within 3 min at 4°C and free Ca^{2+} and $\text{Mg}^{2+} < 1 \text{ nM}$ (Fig. 3A). Dissociation of the [^3H]IP $_3$ -receptor equilibrium complex by addition of a 100-fold excess of either ice-cold assay buffer or unlabeled IP $_3$ results in rapid, biphasic

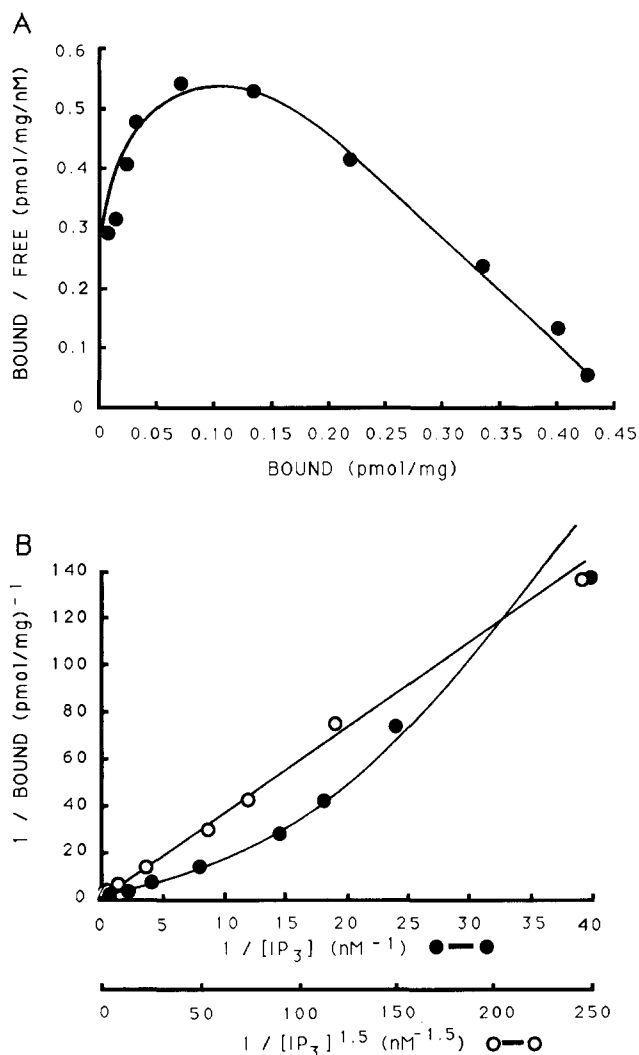


Fig. 2. RBL cell [^3H]IP $_3$ binding sites display multiple affinity states. (A) Scatchard analysis of [^3H]IP $_3$ binding from 0.025 to 10 nM. The experiment is performed by adding 0.025 to 10 nM [^3H]IP $_3$ to RBL cell microsomes and measuring specific binding under equilibrium conditions. Non-specific binding is determined for each IP $_3$ concentration. The free Ca^{2+} and Mg^{2+} concentrations are $< 1 \text{ nM}$. (B) Double-reciprocal plot of IP $_3$ concentration vs. amount [^3H]IP $_3$ specifically bound. The values are derived from the Scatchard plot in (A). The curvilinear plot (●) corresponds to the reciprocal IP $_3$ concentration (upper abscissa). The straight line (○) corresponds to the reciprocal of the IP $_3$ concentration raised to the 1.5 power (lower abscissa). The points in both A & B are mean values of a single representative experiment performed in duplicate and repeated once with similar results.

dissociation (Fig. 3B); the corresponding rate constants are summarized in Table I. The association rate constant k_{+1} is calculated by the relationship

$$k_{+1} = (k_{\text{obs}} - k_{-1}) / [\text{L}]$$

where k_{-1} is the dissociation rate constant determined from Fig. 3B and $[\text{L}]$ is the [^3H]IP $_3$ concentration. When dissociation is measured by dilution, two K_d values can be calculated from the rate constants for the binding of [^3H]IP $_3$ (2.8 and 0.026 nM). The calculated

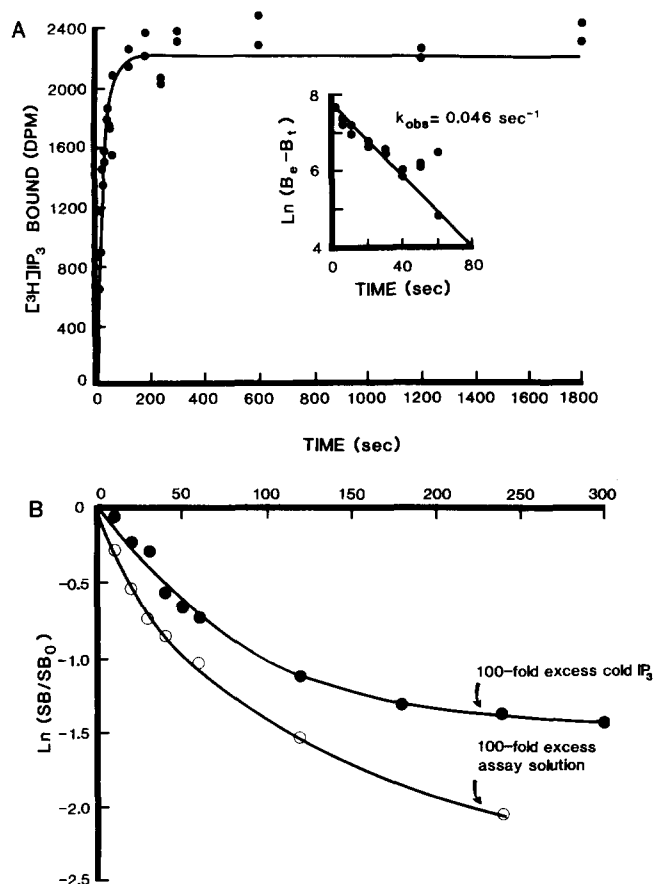


Fig. 3. The association and dissociation of [^3H]IP $_3$ binding. (A) Time course of association of [^3H]IP $_3$ (0.36 nM) to its binding site (Ca^{2+} and $\text{Mg}^{2+} < 1$ nM). Inset: transformation of association binding data as determined by the computer program ENZFITTER. B_t is specific binding at time t , B_e is the binding at equilibrium, and k_{obs} is calculated from the slope. (B) Time-course of dissociation of [^3H]IP $_3$ initiated by adding a 100-fold excess of unlabeled IP $_3$ (●) or of ice-cold assay solution (○) and then determining the amount of residual [^3H]IP $_3$ bound to its receptor. SB_0 is the specific binding at time 0 and SB is specific binding at time t . Both A and B are single experiments performed in duplicate and are representative of two separate experiments. The duplicate values are shown in (A). For clarity, only the mean values are given in (B).

K_d based on the rapid component of dissociation (Table I) is in excellent quantitative agreement with the apparent K_d from equilibrium binding studies per-

formed in the range of 0.4 to 10 nM IP $_3$ (Fig. 1). The k_{-1} values calculated when [^3H]IP $_3$ is dissociated from the receptor complex by competition with unlabeled IP $_3$ are significantly slower than those obtained by the dilution method, and result in calculated K_d values which are markedly lower than those predicted by equilibrium experiments (Table I). Extrapolation of the y-intercepts from linearized dissociation curves (from dilution experiments) show that the low affinity conformational state is more prevalent than the high-affinity conformational state by a ratio of 3:1 (mean of two separate experiments).

Selectivity of the [^3H]IP $_3$ binding site

The selectivity of [^3H]IP $_3$ binding to its microsomal receptor is demonstrated in Fig. 4. Inositol 2,4,5-trisphosphate ($\text{IC}_{50} = 21.4 \pm 1.4$ nM) a synthetic inositol phosphate, and inositol 1,4-bisphosphate ($\text{IC}_{50} = 1.3 \pm 0.17$ μM), a hydrolytic product of IP $_3$, have 9- and 560-fold less affinity for displacing [^3H]IP $_3$ binding, respectively, when compared to IP $_3$ ($\text{IC}_{50} = 2.3 \pm 0.16$ nM). Low molecular weight heparin, a potent inhibitor of IP $_3$ binding [36], inhibits [^3H]IP $_3$ binding in RBL cell tumor tissue with an IC_{50} of 32 ± 1.7 μM . This inhibition of [^3H]IP $_3$ binding by low molecular weight heparin is dependent on the presence of the sulfate groups since the IC_{50} for de-sulfated heparin is > 600 μM (unpublished data). ATP (Mg^{2+} salt) is able to reduce the binding of [^3H]IP $_3$ to its binding site ($\text{IC}_{50} = 228 \pm 24$ μM) at concentrations of ATP that are lower than the amount of ATP found in RBL [26] and mast cells [37]. The Hill numbers derived from the data from Fig. 4 (see figure legend) do not differ significantly from unity, implying that no cooperative interactions exist between the agents tested and the IP $_3$ receptor under these conditions.

Effect of free Ca^{2+} on the binding of [^3H]IP $_3$ to RBL cell microsomes

The free ionized Ca^{2+} concentration has been shown to have a modulatory influence on the IP $_3$ receptor in different cell preparations. In some cases Ca^{2+} inhibits

TABLE I

The rate constants for the association and dissociation of [^3H]IP $_3$ binding are dependent on the method of dissociation

The rate constants are calculated from the transformations of kinetic association and dissociation experiments (Fig. 3). The values \pm S.E. are from experiments performed with similar concentrations of [^3H]IP $_3$. k_{obs} (from Fig. 3A, inset) and k_{-1} (derived from data points in Fig. 3B) are calculated using the nonlinear regression program ENZFITTER. These experiments were repeated once with similar results.

Method of dissociation	k_{obs} (s^{-1})	k_{-1} (s^{-1})	k_{+1} ($\text{nM}^{-1}\text{s}^{-1}$)	K_d (nM)
Dilution	0.044 ± 0.005	0.003 ± 0.0007 0.039 ± 0.0088	0.114 0.014	0.026 2.8
100 \times unlabeled IP $_3$	0.044 ± 0.005	0.001 ± 0.0002 0.028 ± 0.0027	0.119 0.044	0.008 0.636

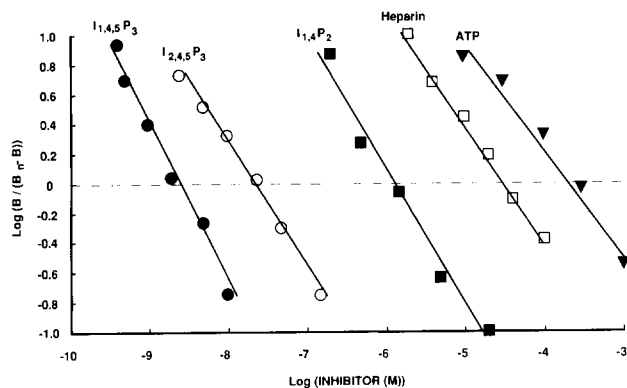


Fig. 4. The inhibition of $[^3\text{H}]\text{IP}_3$ binding by inositol polyphosphates, LMW heparin, and ATP (Mg^{2+} salt). Data are presented as the Hill transformation of inhibition binding experiments where B is occupancy of $[^3\text{H}]\text{IP}_3$ at each inhibitor concentration and B_n is occupancy in the presence of a non-saturating amount of $[^3\text{H}]\text{IP}_3$ in the absence of inhibitor. The correlation coefficients are >0.99 for every plot. Hill numbers are 1.1 ± 0.1 for IP_3 , 0.8 ± 0.04 for inositol 2,4,5-trisphosphate, 0.9 ± 0.1 for inositol 1,4-bisphosphate, 0.8 ± 0.03 for LMW heparin, and 0.9 ± 0.05 for ATP. The molecular weight of heparin is between 4000 and 6000 with an mean value of 5000 used for plotting the data. The data points are mean values of single representative experiments performed in duplicate and replicated at least twice with similar results.

IP_3 binding [4,17,19] while in other cells, Ca^{2+} enhances the binding of IP_3 to its receptor [14]. In RBL cells, Ca^{2+} has both enhancing and inhibitory effects on the binding of $[^3\text{H}]\text{IP}_3$ (0.4 nM) to RBL cell microsomal membranes. With increasing concentrations of free ionized Ca^{2+} up to $10 \mu\text{M}$ there is a modest (approx. 30%) enhancement of specific binding, while a marked inhibition is observed at concentrations of $\text{Ca}^{2+} > 10 \mu\text{M}$ (Fig. 5). Enhancement of $[^3\text{H}]\text{IP}_3$ binding by Ca^{2+} is not due to an increase in affinity but possibly is the result of an increase in the binding capacity of the preparation since the B_{max} increases almost 2-fold with $10 \mu\text{M}$ Ca^{2+} (Table II).

Association rate studies performed at $100 \mu\text{M}$ and $300 \mu\text{M}$ Ca^{2+} reveal that the inhibition of $[^3\text{H}]\text{IP}_3$ binding to microsomal membranes in high concentrations of Ca^{2+} is due to an unstable $[^3\text{H}]\text{IP}_3$ -receptor equilibrium complex (Fig. 6). The association of the binding of $[^3\text{H}]\text{IP}_3$ is characterized by an initial increase in specific binding that reaches a plateau briefly and then declines over the course of the experiment. The rate of association for $[^3\text{H}]\text{IP}_3$ with its binding site in the presence of $300 \mu\text{M}$ Ca^{2+} is faster compared to the association rate in $100 \mu\text{M}$ Ca^{2+} ; the reason for this finding is not known. The instability of the equilibrium at high Ca^{2+} is not the result of a non-specific effect of a large concentration of cations since Mg^{2+} up to 2 mM in concentration has no effect on the binding of $[^3\text{H}]\text{IP}_3$ to its receptor nor on the stability of the equilibrium (unpublished data). Further, the instability does not appear to be due to the binding of Ca^{2+}

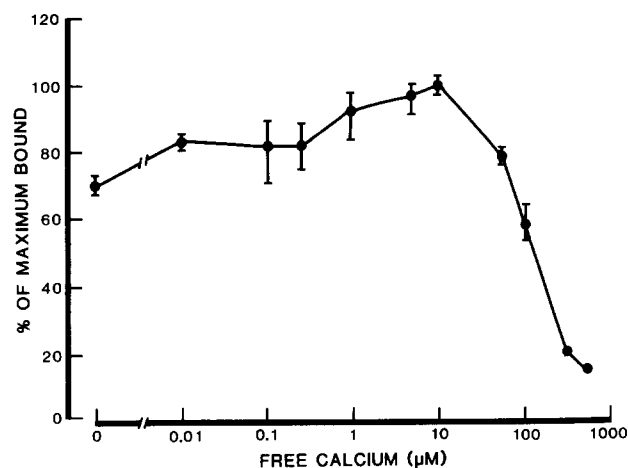


Fig. 5. The effect of the free Ca^{2+} concentration on equilibrium binding of $[^3\text{H}]\text{IP}_3$. The results are the mean of two representative experiments each performed in duplicate at pH 8 and are expressed as a percent of maximal specific binding at $10 \mu\text{M}$ Ca^{2+} (ranging between 0.10 and 0.19 pmol/mg protein). The bars represent the range of values in the two experiments. When bars are not present, the range falls within the area of the symbol.

TABLE II

The binding of $[^3\text{H}]\text{IP}_3$ to RBL cell microsomal membranes is enhanced by free Ca^{2+} up to $10 \mu\text{M}$

Saturation binding experiments are performed with 0.3–0.4 nM $[^3\text{H}]\text{IP}_3$ in the presence of different concentrations of free Ca^{2+} . The values from these experiments are expressed as a mean \pm S.E. These experiments were performed twice with similar results each time.

Free Ca^{2+} (μM)	app K_d (nM)	B_{max} (pmol/mg protein)
0	1.12 ± 0.10	0.9 ± 0.05
1	1.22 ± 0.07	1.47 ± 0.05
10	1.04 ± 0.11	1.62 ± 0.10

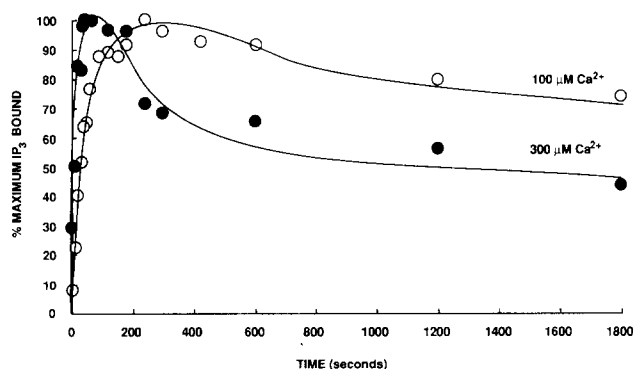


Fig. 6. The association $[^3\text{H}]\text{IP}_3$ binding in the presence of 100 and $300 \mu\text{M}$ Ca^{2+} . Time course of association of $[^3\text{H}]\text{IP}_3$ (0.5 nM) to its binding site in the presence of $100 (\circ)$ or $300 \mu\text{M}$ Ca^{2+} (\bullet). The results are expressed as a percentage of the maximal amount of specific binding that occurred over the course of the experiment (0.07 pmol/mg protein in $100 \mu\text{M}$ Ca^{2+} and 0.09 pmol/mg protein in $300 \mu\text{M}$ Ca^{2+}). The data points are mean values from duplicate samples.

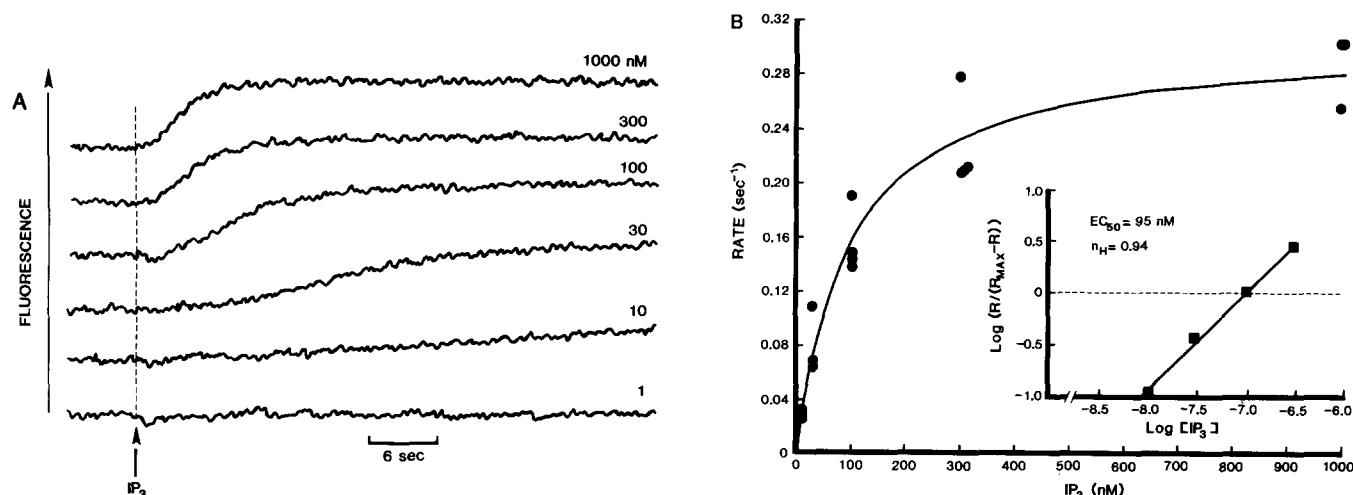


Fig. 7. The rate of Ca²⁺ release from internal stores by IP₃. (A) Representative traces from a single experiment are shown. Permeabilized cells are stimulated with IP₃ (1, 10, 30, 100, 300, and 1000 nM) at the time indicated by the arrow. The fractional change of fluo-3 bound to Ca²⁺ ranges from 0.01 to 0.05. Fluorescence of fluo-3 did not change with the addition of IP₃ to cuvettes containing either saline solution alone or non-permeabilized cells. (B) The Ca²⁺ efflux rate constants (s⁻¹) for the initial release of Ca²⁺ after IP₃ stimulation are determined by taking the reciprocal of the time required for half-maximal release of Ca²⁺. Inset: Hill plots of the efflux rates. R is the efflux rate constant, and R_{\max} is the efflux rate constant at maximal response as determined by the computer program ENZFITTER (0.3081 ± 0.0159 s⁻¹) for this experiment. Only points between 10 and 90% of maximal response are included for analysis. This experiment was performed twice with similar results.

to IP₃ since inhibition binding experiments measuring displacement of [³H]IP₃ by unlabeled IP₃ in the presence of < 0.001, 1, 10, and 100 μM Ca²⁺ do not result in significantly different IC₅₀ values for IP₃ (mean IC₅₀ values of 2.4, 1.9, 2.3, 2.2 nM, respectively, $n = 2$).

Correlation between binding and Ca²⁺ release at nM concentrations of IP₃

IP₃ induces the release of Ca²⁺, measured with fluo-3, from intracellular stores in streptolysin O-permeabilized RBL cells (Fig. 7A). To minimize the amount of Ca²⁺ uptake by intracellular stores following stimulation with IP₃, ATP and Mg²⁺ are not present in the saline solution. ATP is also excluded since it inhibits the binding of IP₃ to its receptor (Fig. 4). Under these conditions the ambient Ca²⁺ concentration is buffered by the permeabilized cells to 192 ± 21 nM. The addition of IP₃ (10–1000 nM) initiates a dose-dependent increase in the rate of Ca²⁺ release from the permeabilized cells (Fig. 7A). The lag time between the addition of IP₃ and the beginning of Ca²⁺ release decreases with increasing concentrations of IP₃ (7 s at 10 nM IP₃ down to 1 s at 1000 nM IP₃). At less than 10 nM concentrations of IP₃, Ca²⁺ release is not detectable. The apparent effective concentration of IP₃ which induces a half-maximal rate of Ca²⁺ release is 100 nM (Fig. 7B, inset) and 60 nM in two separate experiments. In Fig. 7B the relationship of Ca²⁺ efflux rate to IP₃ concentration is hyperbolic, which indicates that the release of Ca²⁺ in response to IP₃ is a simple bimolecular reaction within the IP₃ concentration range of 10–1000 nM. The simple bimolecular reaction corresponds well to the Hill number derived from the Ca²⁺

efflux rates, $n_H = 0.94$ (Fig. 7B, inset) and 0.86 in two separate experiments, and to the single class of binding sites found with Scatchard analysis of IP₃ equilibrium binding data when IP₃ is in the nM concentration range (Fig. 1).

Discussion

From RBL cell solid tumors, we have prepared a microsomal fraction which is enriched in [³H]IP₃ binding activity. The low nM affinity of the receptor for IP₃ and the presence of a single class of binding sites, when the IP₃ concentration is between 0.5 and 10 nM, are observed in both the rapid filtration (Fig. 1) and centrifugation assays and are consistent with those reported from endocrine [8,9], hepatic [12], and smooth muscle [7] membrane preparations. The IP₃ binding site shows selectivity over other inositol phosphates and ATP (Fig. 4). Heparin, an inhibitor of [³H]IP₃ binding to cerebellar [4], and hepatocyte microsomes [38], also inhibits [³H]IP₃ binding to RBL cell microsomal membranes (Fig. 4). The increase in total [³H]IP₃ binding in RBL cell microsomes observed with increasing pH is consistent with findings in cerebellar membranes [4] and other tissues [7,10,17].

Varying the free ionized Ca²⁺ concentration from < 1 nM to 10 μM has a 30% enhancing effect on [³H]IP₃ binding to RBL cell microsomal membranes (Fig. 5). However, if only the physiological range of Ca²⁺ concentrations (from 0.1 to 1 μM) is considered, [³H]IP₃ binding is increased by 9%. This increase is not substantial when compared to the findings of Pietri

and co-workers who show with hepatocyte plasma membrane fractions that IP_3 binding is enhanced approximately 8-fold when the Ca^{2+} concentration is increased from concentrations of $< 100 \text{ nM}$ to $\geq 1 \text{ }\mu\text{M}$ [14]. This enhancement of binding is due to a shift in the receptor from a low- to a high-affinity binding state for IP_3 . Interestingly, this shift to high affinity binding is correlated with the inhibition of IP_3 -induced Ca^{2+} release from permeabilized hepatocytes [14]. We find that the modest enhancement of $[^3\text{H}]\text{IP}_3$ binding to RBL cell microsomes by Ca^{2+} up to $10 \text{ }\mu\text{M}$ is not due to a change in the affinity of the receptor for IP_3 but is the result of an increase in the binding capacity of the preparation since the B_{max} increases almost 2-fold with $10 \text{ }\mu\text{M}$ Ca^{2+} (Table II).

Concentrations of free Ca^{2+} greater than $10 \text{ }\mu\text{M}$ decrease the binding of $[^3\text{H}]\text{IP}_3$ to RBL cell microsomal membranes (Fig. 5). Inhibition of $[^3\text{H}]\text{IP}_3$ binding to hepatic microsomes [11] and platelet membrane vesicles [17] by μM concentrations of Ca^{2+} has also been reported. From association experiments (Fig. 6) it is evident that $[^3\text{H}]\text{IP}_3$ never reaches a stable equilibrium with the microsomal receptor when the free Ca^{2+} concentration is 100 or $300 \text{ }\mu\text{M}$. Our finding of an unstable equilibrium in $[^3\text{H}]\text{IP}_3$ binding may explain why in some cells, IP_3 -induced Ca^{2+} release from intracellular stores is inhibited when the free Ca^{2+} concentration is $10 \text{ }\mu\text{M}$ or greater [39–41]. The mechanism responsible for the unstable equilibrium is not known, but our evidence suggests that it is not due to decreased $[^3\text{H}]\text{IP}_3$ concentrations through increased 5-phosphomonoesterase activity for several reasons. First, this enzyme is not activated by Ca^{2+} [4,35,39], but by Mg^{2+} , which is not present in the assay solution and has a K_m for hydrolyzing IP_3 near $20 \text{ }\mu\text{M}$ [34,35]. Given the low (0.5 nM) $[^3\text{H}]\text{IP}_3$ concentration present in our binding assays, IP_3 degradation is most likely insignificant. Second, the microsomal membranes are washed once and the binding assays are performed in low temperatures which should ensure minimal influences from any phosphatase or proteinase activity [34,35]. Third, the presence of Mg^{2+} , up to 2 mM , (with $\text{Ca}^{2+} < 1 \text{ nM}$) in separate equilibrium binding experiments did not affect specific binding, arguing against an effect of phosphatases in any of the binding assays performed with RBL cell microsomal membranes. In contrast, Sasaguri and co-workers have shown in smooth muscle cells that maximal activation of this phosphatase can occur in the presence of high ($> 1 \text{ }\mu\text{M}$) Ca^{2+} concentrations but in those experiments 2 mM Mg^{2+} was also present [42]. Additional $[^3\text{H}]\text{IP}_3$ association binding experiments performed with permeabilized RBL cells in $500 \text{ }\mu\text{M}$ $\text{Ca}^{2+} \pm 1 \text{ mM}$ Mg^{2+} demonstrate that the observed instability of the IP_3 -receptor complex is not enhanced by Mg^{2+} , as would be expected if there is increased hydrolysis of

$[^3\text{H}]\text{IP}_3$, but instead the instability is actually diminished (unpublished data).

Another possibility to consider is that instead of enhancing degradation of IP_3 , increased concentrations of Ca^{2+} may lead to the formation of IP_3 . A recent report by Mignery and co-workers demonstrated that in cerebellar microsomes, calcium concentrations greater than $10 \text{ }\mu\text{M}$ led to decreased binding of IP_3 to its receptor [43]. They determined that this was due to increased PIP_2 hydrolysis which led to increased IP_3 production. We cannot rule out that when free Ca^{2+} is greater than $10 \text{ }\mu\text{M}$, IP_3 production may be increased in the RBL cell microsomal preparation, thus giving the appearance of decreased $[^3\text{H}]\text{IP}_3$ binding. Whatever the mechanism by which Ca^{2+} affects the IP_3 receptor might be, these data taken together suggest that Ca^{2+} at concentrations which could be attained within localized regions of the IP_3 receptor channel complex may directly or indirectly influence the kinetics of IP_3 binding to its receptor site by allosteric modulation.

Although the characteristics of $[^3\text{H}]\text{IP}_3$ equilibrium binding to RBL cell microsomes are very similar to other non-neuronal cell types in terms of affinity of the receptor for IP_3 , its selectivity over other analogues, and its sensitivity to modulators such as pH and Ca^{2+} concentration, the kinetic binding studies presented here document a novel observation about the $[^3\text{H}]\text{IP}_3$ binding site in nonexcitable cells. From dissociation studies, we observe a biphasic dissociation of the $[^3\text{H}]\text{IP}_3$ -receptor complex by either competition with unlabeled IP_3 or by dilution with excess assay solution (Fig. 3B). The appearance of biphasic dissociation can indicate the possibility either of two independent classes of binding sites for IP_3 or of cooperative interactions when IP_3 binds. The slower dissociation of $[^3\text{H}]\text{IP}_3$ binding by competition with excess unlabeled IP_3 suggests that the biphasic dissociation may be due to allosteric interactions between the ligand and its binding sites [44] on the channel oligomers. In addition, Scatchard analysis of $[^3\text{H}]\text{IP}_3$ equilibrium binding experiments performed with pM to nM concentrations of $[^3\text{H}]\text{IP}_3$ shows a convex relationship (Fig. 2A), supporting the idea that an allosteric mechanism may be involved in IP_3 -receptor binding in RBL cells. However, the Hill number of 1.5, derived from these equilibrium binding experiments indicates that any allosterism involved in IP_3 -receptor interactions would be weak. This may suggest that the complex binding behavior observed in the presence of pM concentrations of $[^3\text{H}]\text{IP}_3$ may be the result of a sequential mechanism that is dependent on IP_3 concentration and may reflect IP_3 -mediated transitions in channel conformation. This mechanism has been proposed to be involved in the interaction of ryanodine with the Ca^{2+} release channel of sarcoplasmic reticulum [45,46], an intracellular re-

ceptor- Ca^{2+} channel complex with structural and functional similarity to the IP_3 receptor. Consistent with this interpretation, Watras and co-workers recently have demonstrated multiple conductance states of the IP_3 -sensitive channel reconstituted in lipid bilayers [47].

Binding studies with cloned cerebellar IP_3 receptor subunits that have deleted transmembrane segments and are in the form of soluble monomers, show that [^3H] IP_3 binds independently to each soluble subunit with a single K_d ranging from 14 to 28 nM in soluble monomers with intact N-terminal regions [48]. This would suggest that IP_3 -receptor interactions are not allosteric. However, this finding does not discount the possibility that as a homotetramer, the IP_3 -receptor binding reaction deviates from mass action since the binding affinity is higher [48] in soluble subunit monomers than in the intact receptor [4]. Thus while it is clear that each monomer of the IP_3 receptor is able to independently bind IP_3 , the nature of this interaction in the native state needs to be resolved.

The binding between IP_3 and its receptor has also been shown to be more complicated than a single binding site model in other non-neuronal tissues. O'Rourke and co-workers report the possibility of either two independent binding sites or cooperativity in the binding of [^3H] IP_3 to platelet membranes [17] in the concentration range of 0.25 to 100 nM [^3H] IP_3 ; however, the cooperativity is negative and only demonstrated under alkaline conditions. Spät and co-workers describe the equilibrium binding of radiolabeled IP_3 to two specific components of liver microsomal membranes; however, kinetic studies performed on the same membrane fraction show that radiolabeled- IP_3 dissociation is from a single class of binding sites [11]. More than one class of binding site for IP_3 in hepatocyte membranes has also been described by Mauger and co-workers [13,14]. Complex interactions in radiolabeled IP_3 binding to its receptor are also introduced depending on pretreatment temperatures and the presence of Ca^{2+} . Finally, the binding of [^3H] IP_3 to a microsomal fraction from peritoneal mast cells can be resolved into two distinct components [16]. The apparent K_d values of the high- and low-affinity binding components are 52 pM and 22 nM, respectively. It is interesting that in the RBL cell microsomal preparation reported here, a binding site having pM affinity is clearly present.

The dissociation curve in Fig. 3B can be resolved into two computer-determined linear components: one due to a rapidly dissociating (low-affinity) site and another to a slowly dissociating (high-affinity) site. The relative number of binding sites determined from the y-intercepts indicates that the ratio of low- to high-affinity sites is on the average 3:1. If all four sites are important for Ca^{2+} release, this would be in agreement with the observation by Meyer and co-workers that the

opening of the IP_3 receptor-channel complex requires the binding of at least three [27] or more [28] molecules of IP_3 .

The affinity of the slowly dissociating component for IP_3 is calculated to be in the pM range (Table I). Since this study (Fig. 7) and others [27,28] have demonstrated that nM concentrations of IP_3 are required to elicit a measurable release of Ca^{2+} from permeabilized RBL cells, the function of this high-affinity site is unclear. In addition, the binding of [^3H] IP_3 to the low-affinity conformational state of the IP_3 receptor with apparent affinity of 1.5 nM occurs at a much lower concentration of IP_3 than is required to elicit half-maximal rates of Ca^{2+} release from intracellular Ca^{2+} stores. In the accompanying paper we present evidence that permeabilized RBL cells, whose soluble cellular constituents are not removed, possess a single class of low-affinity IP_3 binding sites. Moreover, the binding affinity to this class of sites is in the approximate range of IP_3 concentrations that induces the half-maximal rate of Ca^{2+} release from IP_3 -sensitive stores (Fig. 7). The differences in binding affinities found between permeabilized RBL cells (companion paper) and microsomal membranes (this study) in no way negate the significance of different conformation states of the IP_3 receptor in the microsomal membrane preparations. Soluble cytosolic factors may be responsible for modulating the activity of the IP_3 receptor in intact cells.

IP_3 -induced Ca^{2+} efflux from permeabilized RBL cells does not show evidence of any cooperative interactions (Fig. 7B) which most notably differs from the finding of a high degree of cooperativity to IP_3 -induced Ca^{2+} release in RBL cells reported by Meyer and co-workers [27,28]. Our analysis of the relationship between Ca^{2+} efflux rate and IP_3 concentration is based on a wide range of IP_3 concentrations (10 to 1000 nM) since in our experimental system, the behavior of IP_3 -induced Ca^{2+} release rate over this concentration range is one of a simple bimolecular reaction (Fig. 7B). Meyer and co-workers also found that the maximal rate of Ca^{2+} efflux is observed when IP_3 is about 1000 nM [28]. However, in calculating the Hill number they used only those rates obtained at the lower nM concentrations of IP_3 where the steep dependence of Ca^{2+} efflux on IP_3 concentration would indicate a highly cooperative interaction and also where the rates of Ca^{2+} efflux are less than 10% of their reported maximal rate.

Cooperative interaction in IP_3 -induced Ca^{2+} release has been found in permeabilized rat hepatocytes [49,50], although, the cooperativity in both cases is much weaker ($n_H = 1.6$ and 1.7, respectively) than what has been reported by Meyer et al. [28] in permeabilized RBL cells. In contrast, there has been no evidence found for a cooperative dependence of IP_3 -induced Ca^{2+} release in brain microsomes [41,47].

RBL cells grown as solid tumors are an excellent source of material for isolation, purification, and characterization of the IP₃ receptor from bone marrow-derived cells. Comparison of the [³H]IP₃ binding properties of the microsomal IP₃ receptor with those of permeabilized cells will provide insights into the mechanisms involved in coordinating ligand-receptor interactions with the functional release of Ca²⁺ from IP₃-sensitive stores in nonexcitable cells.

Acknowledgments

This work was supported in part by Biomedical Research Support Grant 90-16 (FCM), National Institute of Health Grant ES05002 (INP), and National Science Foundation Graduate Fellowship (PECH).

References

- 1 Streb, H., Irvine, R.F., Berridge, M.J. and Schulz, I. (1983) *Nature* 306, 67-69.
- 2 Ferris, C.D., Haganir, R., L., Supattapone, S. and Snyder, S.H. (1989) *Nature* 342, 87-89.
- 3 Furuichi, T., Yoshikawa, S., Miyawaki, A., Wada, K., Maeda, N. and Mikoshiba, K. (1989) *Nature* 342, 32-38.
- 4 Worley, P.F., Baraban, J.M., Supattapone, S., Wilson, V.S. and Snyder, S.H. (1987) *J. Biol. Chem.* 262, 12132-12136.
- 5 Supattapone, S., Worley, P.F., Baraban, J.M. and Snyder, S.H. (1988) *J. Biol. Chem.* 263, 1530-1534.
- 6 Maeda, N., Kawasaki, T., Nakade, S., Yokota, N., Taguchi, T., Kasai, M. and Mikoshiba, K. (1991) *J. Biol. Chem.* 266, 1109-1116.
- 7 Chadwick, C.C., Saito, A. and Fleischer, S. (1990) *Proc. Natl. Acad. Sci. USA* 87, 2132-2136.
- 8 Baukal, A.J., Guillemette, G., Rubin, R., Spät, A. and Catt, K.J. (1985) *Biochem. Biophys. Res. Commun.* 133, 532-538.
- 9 Guillemette, G., Balla, T., Baukal, A.J. and Catt, K.J. (1987) *Proc. Natl. Acad. Sci. USA* 84, 8195-8199.
- 10 Rossier, M.F., Capponi, A.M. and Vallotton, M.B. (1989) *J. Biol. Chem.* 264, 14078-14084.
- 11 Spät, A., Fabiato, A. and Rubin, R.P. (1986) *Biochem. J.* 233, 929-932.
- 12 Guillemette, G., Balla, T., Baukal, A.J. and Catt, K.J. (1988) *J. Biol. Chem.* 263, 4541-4548.
- 13 Mauger, J.-P., Claret, M., Pietri, F. and Hilly, M. (1989) *J. Biol. Chem.* 264, 8821-8826.
- 14 Pietri, F., Hilly, M. and Mauger, J.-P. (1990) *J. Biol. Chem.* 265, 17478-17485.
- 15 Spät, A., Bradford, P.G., McKinney, J.S., Rubin, R.P. and Putney, J.W., Jr. (1986) *Nature* 319, 514-516.
- 16 Yoshii, N., Mitsunobu, M. and Tasaka, K. (1988) *Immunopharmacology* 16, 107-113.
- 17 O'Rourke, F. and Feinstein, M.B. (1990) *Biochem. J.* 267, 297-302.
- 18 Bradford, P.G. and Autieri, M. (1991) *Biochem. J.* 280, 205-210.
- 19 Joseph, S.K., Rice, H.L. and Williamson, J.R. (1989) *Biochem. J.* 258, 261-265.
- 20 Willcocks, A.L., Cooke, A.M., Potter, B.V.L. and Nahorski, S.R. (1987) *Biochem. Biophys. Res. Commun.* 146, 1071-1078.
- 21 Barsumian, E.L., Isersky, C., Petrino, M.G. and Siraganian, R.P. (1981) *Eur. J. Immunol.* 11, 317-323.
- 22 Cunha-Melo, J.R., Dean, N.M., Moyer, J.D., Maeyama, K. and Beaven, M.A. (1987) *J. Biol. Chem.* 262, 11455-11455.
- 23 Beaven, M.A., Rogers, J., Moore, J.P., Hesketh, T.R., Smith, G.A. and Metcalfe, J.C. (1984) *J. Biol. Chem.* 259, 7129-7136.
- 24 Mohr, F.C. and Fewtrell, C. (1987) *J. Cell Biol.* 104, 783-792.
- 25 Fewtrell, C. and Metzger, H. (1981) in *Biochemistry of the Acute Allergic Reactions* (Becker, E.L., Simon, A.J. and Austen, K.F., eds), pp. 295-314, Alan R. Liss, New York.
- 26 Mohr, F.C. and Fewtrell, C. (1987) *J. Biol. Chem.* 262, 10638-10643.
- 27 Meyer, T., Holowka, D. and Stryer, L. (1988) *Science* 240, 653-656.
- 28 Meyer, T., Wensel, T. and Stryer, L. (1990) *Biochemistry* 29, 32-37.
- 29 Taugog, J.D., Fewtrell, C. and Becker, E.L. (1979) *J. Immunol.* 122, 2150-2153.
- 30 Lowry, O.H., Rosebrough, N.J., Farr, A.L. and Randall, R.J. (1951) *J. Biol. Chem.* 193, 265-275.
- 31 Fabiato, A. (1988) *Methods Enzymol.* 157, 378-401.
- 32 Minta, A., Kao, J.P. and Tsien, R.Y. (1989) *J. Biol. Chem.* 264, 8171-8178.
- 33 Tsien, R.Y., Pozzan, T. and Rink, T.J. (1982) *J. Cell Biol.* 94, 325-334.
- 34 Guillemette, G., Balla, T., Baukal, A.J., Spät, A. and Catt, K.J. (1987) *J. Biol. Chem.* 262, 1010-1015.
- 35 Downes, C.P., Mussat, M.C. and Michell, R.H. (1982) *Biochem. J.* 203, 169-177.
- 36 Ghosh, T.K., Elis, P.S., Mullaney, J.M., Ebert, C.L. and Gill, D.L. (1988) *J. Biol. Chem.* 263, 11075-11079.
- 37 Diamant, B. (1975) *Archs. Allergy Appl. Immun.* 49, 155-171.
- 38 Tones, M.A., Bootman, M.D., Higgins, B.F., Lane, D.A., Pay, G.F. and Lindahl, U. (1989) *FEBS Lett.* 252, 105-108.
- 39 Jean, T. and Klee, C.B. (1986) *J. Biol. Chem.* 261, 16414-16420.
- 40 Zhao, H. and Muallem, S. (1990) *J. Biol. Chem.* 265, 21419-21422.
- 41 Finch, E.A., Turner, T.J. and Goldin, S.M. (1991) *Science* 252, 443-446.
- 42 Sasaguri, T., Hirata, M. and Kuriyama, H. (1985) *Biochem. J.* 231, 497-503.
- 43 Mignery, G.A., Johnston, P.A. and Südhof, T.C. (1992) *J. Biol. Chem.* 267, 7450-7455.
- 44 Weiland, G.A. and Molinoff, P.B. (1981) *Life Sci.* 29, 313-330.
- 45 Pessah, I.N. and Zimányi, I. (1991) *Mol. Pharm.* 39, 679-689.
- 46 Carroll, S., Skarmeta, J.G., Yu, X., Collins, K.D. and Inesi, G. (1991) *Arch. Biochem. Biophys.* 290, 239-247.
- 47 Watras, J., Bezprozvanny, I. and Ehrlich, B.E. (1991) *J. Neurosci.* 11, 3239-3245.
- 48 Miyawaki, A., Furuichi, T., Ryou, Y., Yoshikawa, S., Nakagawa, T., Saitoh, T. and Mikoshiba, K. (1991) *Proc. Natl. Acad. Sci. USA* 88, 4911-4915.
- 49 Champeil, P., Combettes, L., Berthon, B., Doucet, E., Orlowski, S. and Claret, M. (1989) *J. Biol. Chem.* 264, 17665-17673.
- 50 Nunn, D.L. and Taylor, C.W. (1990) *Biochem. J.* 270, 227-231.